CYANOGEN JETS AND THE ROTATION STATE OF COMET MACHHOLZ (C/2004 Q2)

Tony L. Farnham[1]
Department of Astronomy, University of Maryland, College Park, MD 20742, USA; farnham@astro.umd.edu

Nalin H. Samarasinha[2]
National Optical Astronomy Observatory, Tucson, AZ 85719, USA; and Planetary Science Institute, Tucson, AZ 85719, USA

Béatrice E. A. Mueller[1]
Planetary Science Institute, Tucson, AZ 85719, USA

and

Matthew M. Knight[1]
Department of Astronomy, University of Maryland, College Park, MD 20742, USA

ABSTRACT

Extensive observations of Comet Machholz (C/2004 Q2) from 2005 February, March, and April were used to derive a number of the properties of the comet's nucleus. Images were obtained using narrowband comet filters to isolate the CN morphology. The images revealed two jets that pointed in roughly opposite directions relative to the nucleus and changed on hourly timescales. The morphology repeated itself in a periodic manner, and this fact was used to determine a rotation period for the nucleus of 17.60 ± 0.05 hr. The morphology was also used to estimate a pole orientation of R.A. $= 50°$, decl. $= +35°$, and the jet source locations were found to be on opposite hemispheres at mid-latitudes. The longitudes are also about $180°$ apart, although this is not well constrained. The CN features were measured to be moving at about 0.8 km s^{-1}, which is close to the canonical value typically quoted for gas outflow. Future modeling of the CN features will be used to improve and extend these results.

Key words: comets: general — comets: individual (Machholz C/2004 Q2)

1. INTRODUCTION

Comet Machholz (C/2004 Q2) was discovered by D. E. Machholz on 2004 August 27 (Machholz et al. 2004). Soon after discovery, it was predicted to become very bright before its perihelion passage on 2005 January 24. It lived up to expectations, reaching naked-eye brightness at about magnitude 3.5 around the time of its closest approach to Earth on January 5 (0.35 AU), but by 2005 April it was fading rapidly as both heliocentric and geocentric distances increased.[3] On 2005 February 9, a rotation period and a pole orientation were announced by Sastri et al. (2005a, 2005b). Their solution was based on modeling of features observed in the dust coma in early and mid-January. They found a rotation period of 9.1 ± 2 hr and a pole at right ascension of $190° \pm 10°$ and declination of $+50° \pm 10°$. From their models, they also found three jets in the southern hemisphere, at latitudes in the ranges of $0°$ to $-15°$, $-35°$ to $-50°$, and $-70°$ to $-78°$.

An accurate measurement of the rotational properties of a comet's nucleus is important because the adopted rotation state can have a significant impact on the interpretation of other observations. For example, the radar albedo and nucleus radius based on radar observations are strongly dependent on the value used for the rotation period and the spin axis orientation (Nolan et al. 2005), and thermal models of the nucleus rely on the ability to distinguish between rapid rotators and slow rotators (e.g., Weissman & Kieffer 1981).

During an observing campaign of comet Tempel 1, we also obtained images of comet Machholz at roughly monthly intervals between 2005 January and June. In mid-January only broadband images were obtained, but they showed little structure, in contrast to the observations of Sastri et al. (2005a). Starting in February, we obtained images using the HB narrowband comet filters (Farnham et al. 2000) to isolate the spatial structure of the gas species and dust in the coma. These images showed strong cyanogen (CN) jets and features that changed on a timescale of hours. These changes were caused by the rotation of the nucleus. After the discovery of these jets in February, a concentrated effort was undertaken in March and April to obtain more complete observations, which could be used to derive the rotation state of the nucleus.

2. OBSERVATIONS

2.1. Observations and Data Reduction

A list of the observing conditions and geometries is given in Table 1. The primary observations that are discussed here were obtained 2005 March 11–14 and 2005 April 9–14 at the Kitt Peak National Observatory (KPNO) 2.1 m telescope using the F3KB CCD (which has 0.19″ pixel^{-1}). On these nights, the comet was at high northern declinations ($\sim$84° in March and $\sim$71° in April) and thus was observable for about 10 hr per night. These windows of visibility provided uninterrupted coverage of long spans of the comet's rotation, helping to reduce the chances of aliasing of the rotational phase from night to night. The observing and geometric conditions were excellent, with typical seeing around 1″ and pixel

FARNHAM ET AL.

UT Date	KPNO Telescope	r_H (AU)	Δ (AU)	Solar Phase Angle (deg)
2005 Jan 16–17	4.0 m	1.21	0.38	45–46
2005 Feb 3–4	2.1 m	1.21–1.22	0.52–0.53	52
2005 Mar 11–14	2.1 m	1.39–1.42	0.88–0.91	45–44
2005 Apr 9–14	2.1 m	1.65–1.70	1.18–1.24	37–36
2005 May 14–17	2.1 m	2.02–2.05	1.61–1.66	30–29
2005 Jun 4–7.............	2.1 m	2.25–2.28	1.94–1.99	27–26

scales of ~125 and ~165 km at the comet in March and April, respectively.

High-resolution observations were also obtained on February 3–4, with a pixel scale of ~70 km, although only a few images were taken. Additional observations were obtained on May 14–17 and June 4–7, but by this time the comet's heliocentric and geocentric distances were increasing, and the structures were affected by a low signal-to-noise ratio (S/N). For the current work, the May and June observations will not be addressed.

Images were obtained using a Harris broadband R filter and the HB narrowband comet filters (Farnham et al. 2000), which isolate the spatial structure of the gas (CN, OH, and C_2) and dust in the coma. The discussion presented here concentrates on the results from the CN filter, with other filters to be discussed in a future paper. The data were reduced using standard procedures. The bias was removed using a combination of the overscan region and a master bias frame. Flat-fielding was performed using dome flats to remove pixel-to-pixel variations across the CCD. Asymmetries in the coma are visible in the reduced CN images from February and March, even with no image enhancements. These asymmetries indicate that there are features present in the coma, likely produced by isolated active areas on the surface. Coma features of this kind are not uncommon, having been observed in comets Halley (e.g., A'Hearn et al. 1986), Hyakutake (e.g., Schleicher & Woodney 2003; Samarasinha et al. 2004), and Hale-Bopp (e.g., Farnham et al. 1998; Lederer et al. 1998; Mueller et al. 1997), among others, and can be used to infer properties of the nucleus.

Typically, the final step in the reduction of CN images is the removal of the continuum to obtain the structure of the pure gas coma. Because the CN filter also captures reflected light from the dust, any structure in the underlying continuum can affect the appearance of the CN structure. In comet Machholz, however, the dust contributes only a few percent of the signal in the CN bandpass, and most of that signal is concentrated in the central peak (from measurements on March 8 and 10; D. G. Schleicher 2006, private communication). This means that the dust contribution is small to start with, and the majority of that contribution is effectively removed using the enhancement technique described in § 2.2. Thus, any remaining contribution will be negligible, and so we chose not to perform a formal removal of the continuum. Additional support for this decision is presented in § 3.

2.2. Image Enhancements

In order to improve the contrast of the features in the inner coma, the bright central peak needs to be removed using enhancement techniques. We typically investigate a number of different methods, each of which may reveal different types of features (Larson & Slaughter 1992; Schleicher & Farnham 2004; Samarasinha et al. 2006b). Using several different techniques also allows us to
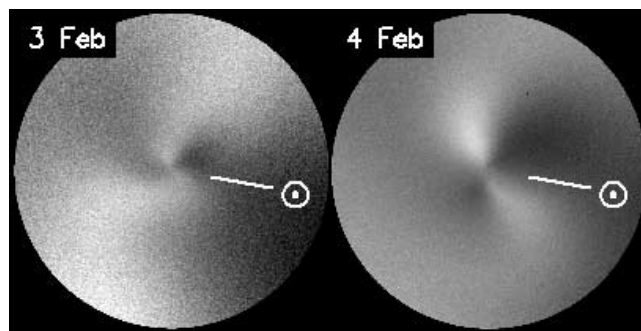

FIG. 1.—CN images of comet Machholz from February 3.169 and 4.272, showing the structure that prompted further follow-up to determine the rotation period. The nucleus is at the center of each image, with two jets extending outward in opposite directions. The images have been enhanced by dividing out the azimuthally averaged radial profile as discussed in the text. (With this processing, circular portions of the image are extracted, leaving the corners black.) The February 3 image is 3.9×10^4 km across, and the February 4 image is 5×10^4 km across; north is up, and east is to the left. The projected sunward direction is marked.

evaluate whether the features are real or if artifacts have been introduced. For the images examined here, we find that division by a simple azimuthal average works well to show the CN morphology. This technique computes the mean value of all pixels at a given distance from the optocenter to generate an average radial profile of the coma. Each pixel is then divided by the average value for its radial distance to improve the contrast of the features. One advantage of this technique is that it uses the image itself to remove the central peak and the radial falloff, requiring no a priori assumptions about the coma shape. It also preserves any azimuthal asymmetries that may exist. This enhancement reveals CN jets that are reminiscent of those seen in comet Halley (A'Hearn et al. 1986). Figure 1 shows two images from February and illustrates how the enhancement reveals the CN features. The difference in morphology on the two days prompted us to obtain follow up observations in subsequent months. (Note that all images are shown with north up and east to the left unless otherwise noted.)

3. COMA MORPHOLOGY

After the CN images from February, March, and April have been enhanced, they clearly show two jets pointing in roughly opposite directions from the nucleus. Motions of these jets are detectable on timescales as short as an hour. The extended features exhibit corkscrew shapes, indicating that material is streaming out of an active source on a rotating nucleus. If a source is at a high latitude, the outflow will spiral outward along the sides of a cone. When the Earth is outside the cone, the jet appears to oscillate back and forth, and the gas will produce the characteristic corkscrew pattern (e.g., Sekanina 1991) observed in these images. Because we see jets in opposite directions, there must be two sources, on opposite hemispheres of the nucleus. Both CN jets remain visible throughout a full rotation cycle, suggesting that their sources remain active even when they are not illuminated. There are times, however, when the jets appear fainter, and this could indicate that the activity is reduced when the active area rotates around the night side of the nucleus, a phenomenon also observed in other comets (e.g., Hale-Bopp; Farnham et al. 1998; Lederer et al. 1998; Samarasinha et al. 1997).

The side boundaries of the corkscrew are the extremes of the oscillation reached by the jets (i.e., the projected edges of the cone) and can be used to constrain some of the nucleus properties. In the February images (Fig. 1) the southeast jet appears to oscillate between position angles (P.A.s) of about $140°$ and $200°$, and
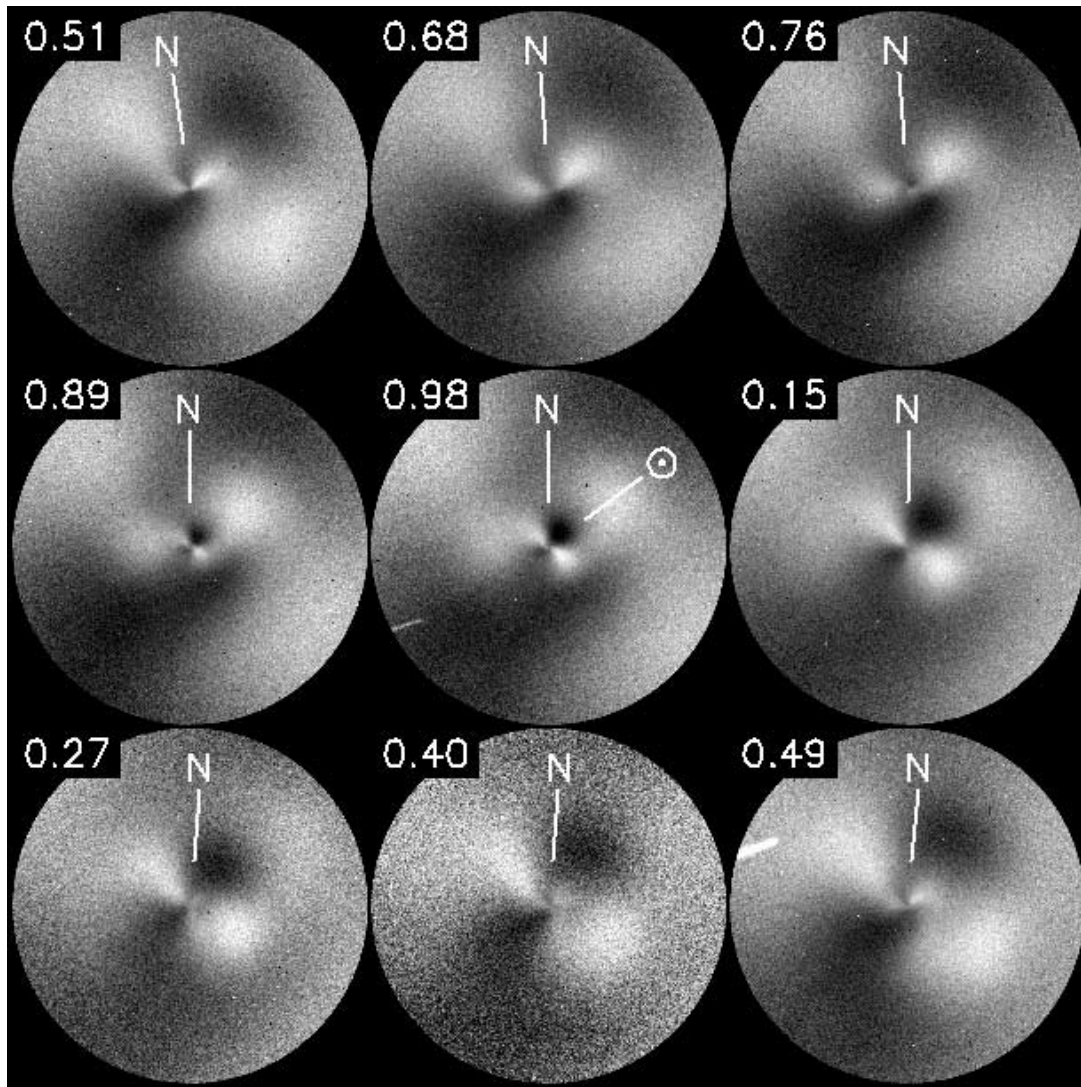
Fɪɢ. 2.—Sequence of CN images from March 11 through 14, phased to a 17.60 hr rotation period. The rotational phase is noted in the top left of each panel, with zero phase defined as March 11.0 UT. The corkscrew shape of the rotating jet to the west is clearly apparent in phases around 0.5. The comet's motion at high northerly declination produced an apparent rotation of the image plane, so for consistency the images have been aligned so that the sunward direction is constant (shown in the center panel). This results in a change in the projected direction of north, which is shown in the individual frames. East is 90° to the left of the north vector. The field of view is about 10^5 km in each panel. The white streaks are star trails. Following the phase sequence from the upper left, the images were obtained on March 11.372, 12.235, 12.288, 13.116, 13.183, 13.312, 14.128, 14.227, and 14.295 UT. See the caption for Fig. 1 for more information.

the northwest jet oscillates between 310° and 30°. There are only a limited number of images from this month, and therefore, the extrema could vary somewhat from this estimate. In March, one jet is bounded by P.A.s 50° and 110° and the other by 220° and 300° (see Fig. 2). In this figure, the corkscrew shape is well defined, especially for the westward feature, in the images obtained at rotational phases around 0.5 (where the phase is noted in the top left corner of each panel). For the April images (Fig. 3), one jet oscillates between P.A.s of 80° and 190° and the other between 260° and 10°. We estimate that the P.A. measurements given here have an uncertainty of 10°–20°.

For comparison, we also looked at the continuum images to evaluate the dust morphology. Figure 4 shows four representative dust images taken in March and enhanced with the same technique used for the CN images. The only feature seen is a fan-shaped "tail," which shows essentially no variation as a function of time or rotational phase. (Compare these images with the CN images at the corresponding phases in Fig. 2.) Because this "tail" is not pointed in the antisolar direction, it is likely that it is the result of

dust grains in the form of a jet. The lack of variability is explained if the dust is moving slowly enough that material from consecutive rotations overlaps and smears out the variations (the same phenomenon was seen in comet Tempel 1; Farnham et al. 2007; Samarasinha et al. 2006a). The fact that this continuum structure is not detected in the CN images, even though the continuum has not been removed, confirms that the dust contribution to the CN images is negligible. Thus, for the purposes of this paper, continuum removal is unnecessary. (The same tests were done for the April images, with the same conclusions.) The lack of detectable changes in the continuum morphology suggests that the dust grains are slow moving, and any rotational variations blend together because they are too close to be resolved in the spatial resolution of the images (e.g., Samarasinha et al. 1997). The dust and its differences from the CN will be explored more fully in a future paper.

4. COMA ANALYSIS

During the examination of the March images, we found that the morphology on March 14 was very similar to that seen ∼69 hr
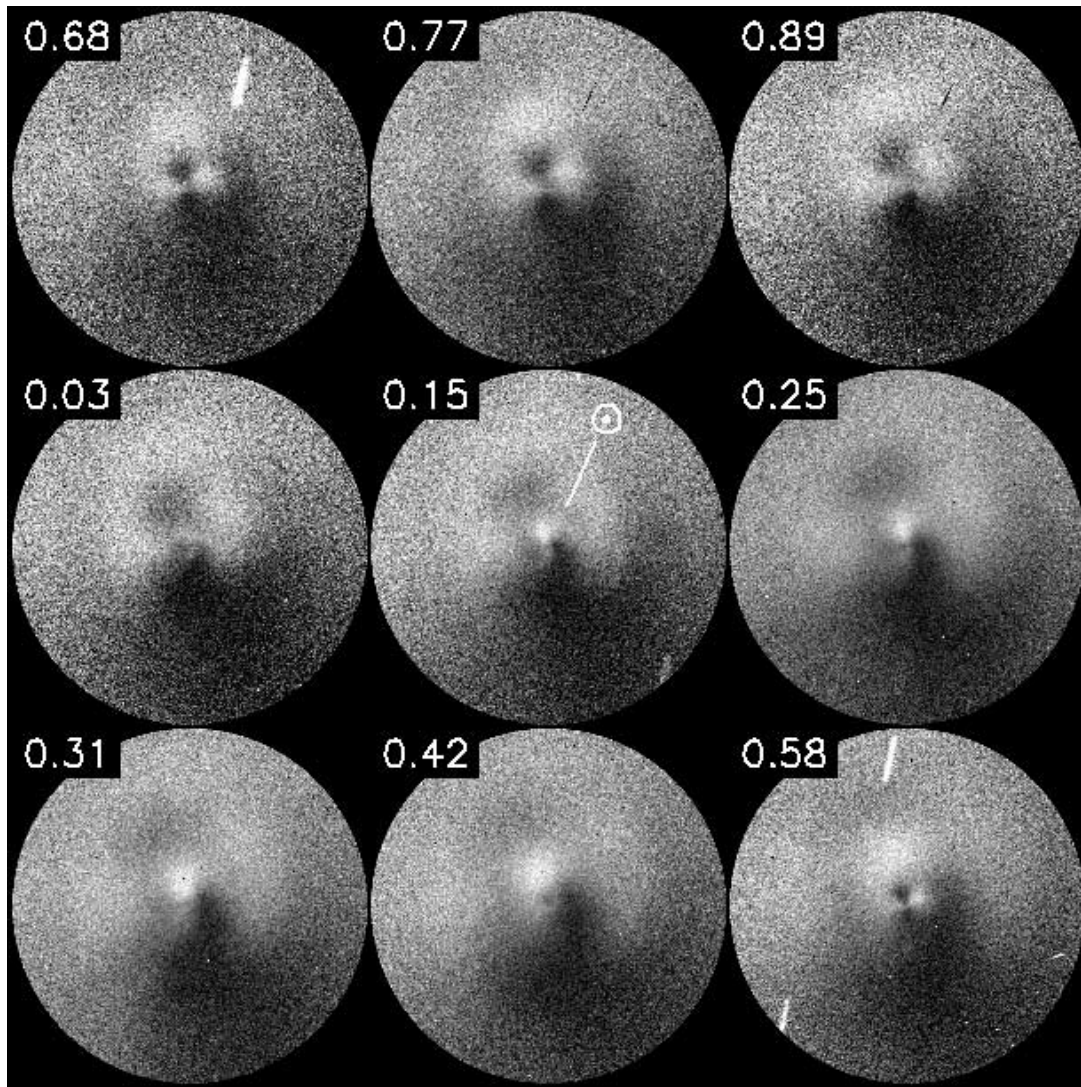
Fig. 3.—Sequence of CN images from April 9 through 14, phased to a 17.60 hr rotation period. The rotational phase is noted in the top left of each panel, with zero phase defined as April 9.0 UT. The projected sunward direction is shown only in the center panel and varies by only $\pm 1°$ through the sequence. The field of view in each panel is about 1.3×10^5 km. North is up, east is to the left, and the white streaks are star trails. Following the phase sequence from the upper left, the images were obtained on April 12.428, 13.229, 13.322, 14.146, 14.246, 9.180, 11.425, 12.239, and 12.356 UT. See the caption for Fig. 1 for more information.

earlier on March 11. Thus, the two observations were obtained at about the same rotational phase, leading to potential periods of about 69, 35, 23, 17, 14, etc., hours, depending on the number of rotations that occurred in the interval. Unfortunately, a unique solution was not immediately obvious from the March images because of limited coverage and because there is no exact match of images during the overlapping phases. The period solution based on morphology was made even more complicated because the comet passed within $6°$ of the celestial north pole, causing the appearance of the comet to change as the image rotated to keep the edges of the CCD aligned with the celestial coordinate frame.

Although we did not find a unique period from the March data, we were able to use the information to obtain targeted observations in April from which we could distinguish between the possible periods. Six nights in April provided more overlap for phasing the observations, and minimal geometry changes allowed us to more easily zero in on the best period. Over the course of 5 days, we were able to capture essentially the same feature on four different occasions: April 9.451, April 10.181, April 12.385, and

April 13.117 UT. These four images, shown in Figure 5, were used to derive a rotation period of the nucleus of 17.60 ± 0.05 hr, a result that was validated by phasing the other images from April.

Any period shorter than this value is precluded by the observations. We have dense temporal coverage on most of the April nights, as shown in Figure 6, where the times of the nightly observations are phased to the 17.60 hr rotation period. From this plot, it is clear that we have the ability to rule out the aliased period of 8.8 hr or any shorter period. First, we have good coverage of the comet spanning almost 9 hr on both April 13 and 14. On these nights, the morphology in the earliest images does not match that in the latest ones, as shown in Figure 7, which in itself rules out any period around 9 hr. Also, if the observations throughout April are phased to an 8.8 hr period, they do not produce a smoothly flowing sequence. For example, if the period was 8.8 hr, then the images labeled 0.77 and 0.25 in Figure 3 should have been obtained at almost the same phase, which is clearly not the case. Any shorter period is ruled out using the same arguments. The fact that the 17.60 hr period produces a smoothly flowing
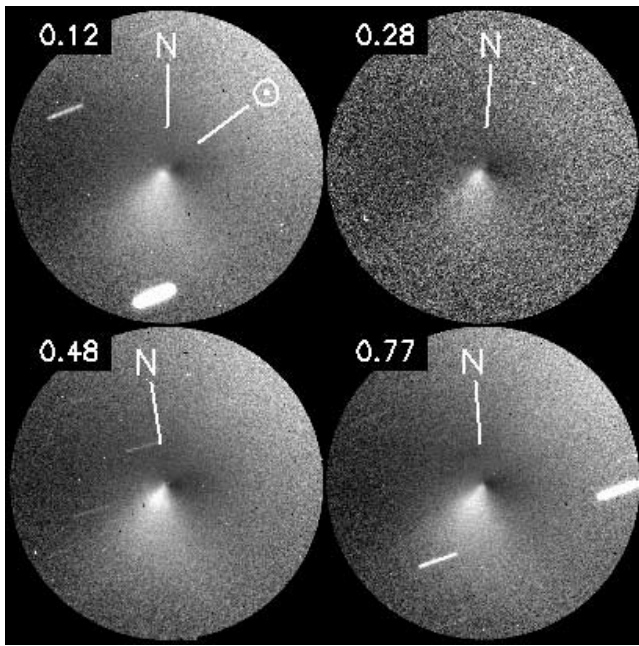
Fig. 4.—Four representative continuum images from March, showing the dust morphology at different rotational phases. These images are paired with the CN images shown in Fig. 2, with the continuum and CN images usually obtained within 30 minutes of each other. As with Fig. 2, the images have been rotated to align the sunward direction (shown in the top left panel), which changes the projected northward direction in each case. In contrast to the CN, the dust structure changes little during a rotation. Following the phase sequence from the top left, the images were obtained on March 13.285, 14.140, 11.353, and 12.300 UT. See the caption for Fig. 2 for more information.
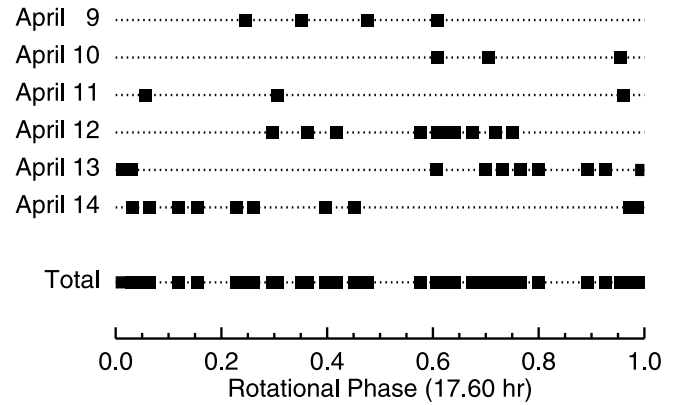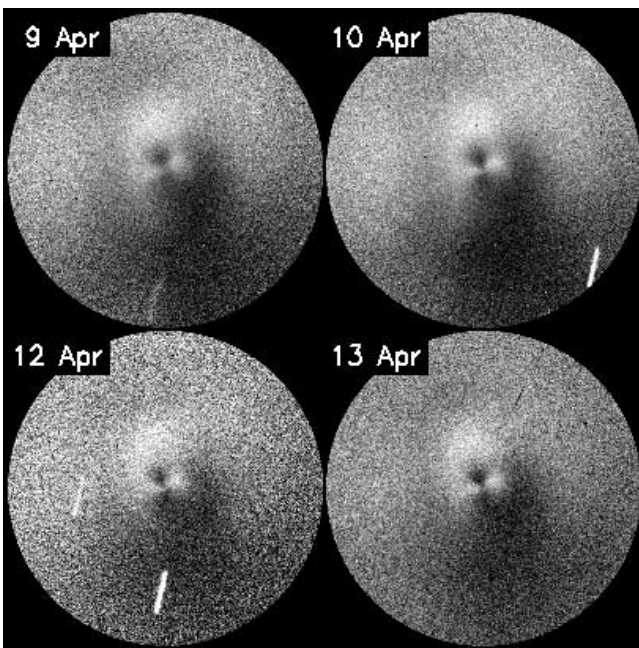

Fig. 5.—Four CN images from April, obtained at the same rotational phase (0.61 ± 0.01 in the sequence shown in Fig. 3). These images from April 9.451, 10.181, 12.385, and 13.117 UT were used to derive the 17.60 hr rotation period of the nucleus. See caption for Fig. 3 for more information.
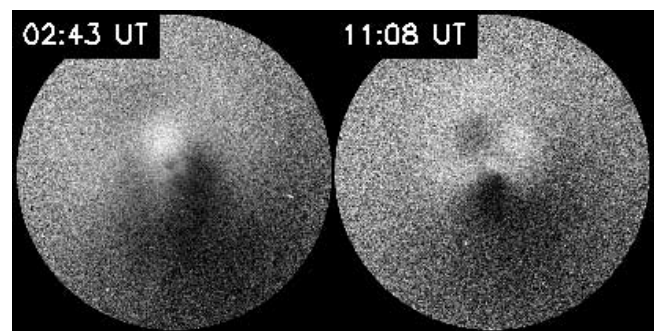

Fig. 6.—Plot showing the times of the April observations, phased to a period of 17.60 hr. Coverage spanning ∼9 hr each on April 13 and 14 precludes any rotation period aliases shorter than 17.60 hr.

sequence when all of the images are phased suggests that this solution is unique.

When corrected for geometric changes, the March data are also consistent with this solution, as shown in Figure 2. (In this figure, the images have been rotated to align the sunward vector at a fixed position, to remove the apparent rotation caused by the comet's high declination.) The last image, at phase 0.49, has a morphology very close to that in the first image at a phase 0.51. The March data can also be used to rule out the ∼9 hr period, in the same way as discussed for the April data. This agreement indicates that there are no dramatic changes in the rotation period between March and April. With our derived rotation period, we were also able to phase the images, both from March and from April, to create "movies" of the rotation that can be used to more easily interpret the evolution of the jets with time.[4]

We next used the coma morphology to estimate the orientation of the spin axis of the nucleus. Our interpretation of the corkscrew effect means that the projected rotation axis must lie at the center of the corkscrew, while the axis actually lies somewhere in the plane defined by the projected axis and the line of sight. Measurements of the P.A. of the axis on multiple dates, observed from different geometries, define individual planes that should intersect along the direction of the pole in inertial space. This assumes that the nucleus is in a state of simple (principal-axis) rotation and that the pole remains fixed in the same orientation for all of the

---

[4] These movies are available at http://www.astro.umd.edu/~farnham/Machholz.

Fig. 7.—Two CN images obtained 8.4 hr apart. The difference in morphology shows that the rotation period cannot be ∼9 hr. The images were obtained on April 14.113 and 14.465 UT (rotational phases 0.972 and 0.452, respectively). See caption for Fig. 3 for more information.
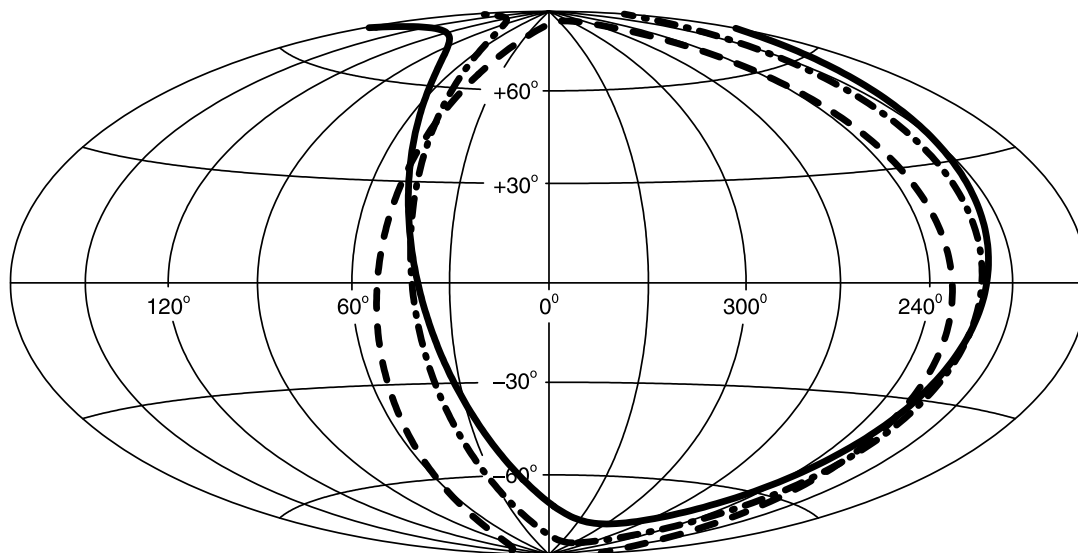
FIG. 8.—Great-circle solutions for the spin axis as measured from February (*dashed line*), March (*dot-dashed line*), and April (*solid line*) and projected onto the celestial sphere in equatorial coordinates (see text). The convergence of the three circles is closest at R.A. $= 50°$ and decl. $= +35°$ (or its $180°$ opposite direction at R.A. $= 230°$ and decl. $= -35°$), which defines the approximate orientation of the pole.

observations. By taking the centers of the extreme jet P.A.s listed in § 3, we can compute the projected pole positions in February ($170°/350°$), March ($80°/260°$), and April ($135°/315°$). Using these values, we can derive the great circles for each observing run and use them to determine the intersection of the planes. With this technique, we compute a pole orientation at R.A. $= 50°$, decl. $= +35°$. Figure 8 shows the projections of the three great circles onto the celestial sphere, with the convergence of the planes around the pole direction. (A second convergence occurs $180°$ away, representing the opposite pole.) In this solution, the right ascension is fairly well constrained ($\pm10°$), but the declination has a large uncertainty and could be off by as much as $30°$. Unfortunately, this solution does not reveal the sense of rotation of the nucleus.

Using the opening angles of the corkscrews, we can estimate the locations of the jet sources on the nucleus. For this task we use the March data because they have a higher S/N, and the interpretation of the jet structure is clearer than in April. In this configuration, the angular width of the jet cone is twice the polar angle to the source, so the jet from $50°$ to $110°$ has a cone angle of $60°$ and thus lies at a latitude around $60°$. The other jet has a cone angle of $80°$, so it lies at a latitude around $50°$ on the opposite hemisphere. Given the uncertainties introduced by diffuse jets, variable solar illumination, and projection effects, we do not claim these latitude determinations to be highly accurate and instead conclude that the jets are located at midlatitudes on their respective hemispheres. Because the jets seem to oscillate in tandem, they are probably about $180°$ apart in longitude, although this probably also has a large uncertainty.

The final item derived from the morphology is the outflow velocity of the CN. Using the March images to minimize the projection effects, we measured the distance from the nucleus to the edges of the corkscrew (where the jet crosses the plane of the sky) as a function of time. The edges move outward about $75''$, or 5×10^4 km during the course of one rotation, which gives a velocity of about 0.8 km s^{-1}. This value is close to, but lower than, the canonical value of 1 km s^{-1} typically cited for gas outflow in comets near 1 AU.

5. DISCUSSION

Our analysis of the CN morphology allowed us to determine a number of nucleus properties, including the rotation period of the nucleus, the orientation of the spin axis, approximate locations of the jets, and the CN outflow velocity. The rotation period was derived from the repeating morphology over 5 days and is model independent.

Our 17.60 hr period is significantly different from the 9.1 hr value derived by Sastri et al. (2005a), but we have shown that a period around 9 hr is inconsistent with our images. The fact that the 17.60 hr period is consistent between the March and April data suggests that the period is unlikely to have evolved from 9.1 hr to 17.6 hr between January and March. Furthermore, the pole orientation derived here is about $90°$ different from the Sastri et al. solution, so we suggest that their interpretation of the dust features is incorrect and the results from their models are not representative of comet Machholz.

Future studies of this comet will focus on the detailed modeling of the CN jets (e.g., comet Hyakutake; Samarasinha et al. 2004) to account for the changes in geometry and the different spatial scales between the images, so all of the data can be incorporated into the analysis. With these improvements, a more precise rotation period can be determined by linking the March and April morphologies. Modeling will also improve the pole solution, to more tightly constrain the declination and to allow an investigation into whether our assumption of simple rotation is correct. It may also be possible to use the times when the jets seem to decrease their activity to define the times at which the sources are in darkness and thus determine the sense of rotation of the nucleus. With the detailed models, the properties of the CN sources will be extended, including better locations, estimates of their sizes and relative production rates, and the effects of solar insolation on their activity levels.

Additional coma properties may be determined using modeling of both the gas and dust. Lifetimes of the CN and its parent species can be constrained, as well as the outflow velocity of the CN parent molecule, the excess velocity of CN, and the outflow

velocity of the dust. Motions of the features can also be used to determine the radiation-pressure accelerations of the CN and the dust particles.

REFERENCES

A'Hearn, M. F., Hoban, S., Birch, P. V., Bowers, C., Martin, R., & Klinglesmith, D. A. 1986, Nature, 324, 649
Farnham, T. L., Schleicher, D. G., & A'Hearn, M. F. 2000, Icarus, 147, 180
Farnham, T. L., Schleicher, D. G., Ford, E., & Blount, E. A. 1998, in First International Conference of Comet Hale-Bopp, ed. M. A'Hearn et al. (Dordrecht: Kluwer), 16
Farnham, T. L., et al. 2007, Icarus, 187, 26
Larson, S. M., & Slaughter, C. M. 1992, in Asteroids, Comets, Meteors 2005, ed. A. Harris & E. Bowell (Houston: Lunar and Planetary Inst.), 337
Lederer, S., Campins, H., Osip, D. J., & Schleicher, D. G. 1998, BAAS, 30, 1063
Machholz, D. E., Garradd, G., & McNaught, R. H. 2004, IAU Circ., 8394, 1
Mueller, B. E. A., Samarasinha, N. H., & Belton, M. J. S. 1997, Earth Moon Planets, 77, 181
Nolan, M. C., Campbell, D. B., Harmon, J. K., Howell, E. S., & Magri, C. 2005, Abstract at IAU Symp. 229, Asteroids, Comets, Meteors (Rio de Janiero)

Samarasinha, N. H., Farnham, T., Mueller, B., Knight, M., Belton, M., A'Hearn, M., & Lisse, C. 2006a, Abstract at Asia Oceania Geosciences Soc., 3rd Annual Meeting (Singapore)
Samarasinha, N. H., Larson, S., & Beshore, E. 2006b, BAAS, 38, 2913
Samarasinha, N. H., Mueller, B. A., & Belton, M. J. 1997, Earth Moon Planets, 77, 189
Samarasinha, N. H., Schleicher, D. G., & Woodney, L. M. 2004, BAAS, 36, 1146
Sastri, J. H., Vasundhara, R., Kuppuswamy, K., & Velu, C. 2005a, IAU Circ., 8480, 3
———. 2005b, IAU Circ., 8484, 1
Schleicher, D. G., & Farnham, T. L. 2004, in Comets II, ed. M. H. Festou, U. Keller, & H. Weaver (Tucson: Univ. Arizona Press), 449
Schleicher, D. G., & Woodney, L. M. 2003, Icarus, 162, 190
Sekanina, Z. 1991, AJ, 102, 350
Weissman, P. R., & Kieffer, H. H. 1981, Icarus, 47, 302